Int. J. Nanosci. Nanotechnol., Vol. 20, No. 3, Sept. 2024, pp. 161-169
DOI: 10.22034/ijnn.2025.2014884.2448

Synthesis of Proper Magnetite Nanoparticles for Preparation of Activated Carbon-Based Nanocomposites as Magnetic Adsorbents

Fathollah Pourfayaz[1,*], **Ali Gholami**[1] **and Farhad Farzan**[2]

[1]Department of Renewable Energies and Environment, Faculty of New Sciences and Technologies, University of Tehran, Tehran, Iran
[2]Chemical Processes Design Research Group, ACECR, Faculty of Engineering, University of Tehran, Tehran, I. R. Iran

(*) Corresponding author: pourfayaz@ut.ac.ir

(Received: 24 November 2023 and Accepted: 08 May 2024)

Abstract

In this study, magnetite, barium hexaferrite, coated, and uncoated iron nanoparticles were prepared. These magnetic nanoparticles were characterized through X-ray diffraction (XRD) analysis, scanning electron microscopy (SEM), and empirical observation of the magnetic properties in practice. The results demonstrated that the barium hexaferrite nanoparticles were magnetically weak and suffered from a cumbersome and costly synthesis process. The uncoated iron nanoparticles were prone to oxidation when exposed to air, and coated iron nanoparticles showed weak magnetic properties. Given their simple synthesis method and strong magnetic properties, magnetite nanoparticles were suitable for magnetizing activated carbon. Toluene adsorption results showed that magnetic adsorbents from activated carbon nanocomposites containing 20% nanoparticles have desirable adsorption.

Keywords: *Activated carbon, Magnetite nanoparticles, Nanoadsorbents, Nanocomposites.*

1. INRODUCTION

The small and nanometric size of particles increases their surface area to volume ratio, and their thermal, electronic, magnetic, and optical properties are better reflected. Although the word "nano-particle" became common when advancements in microscopy led us to observe them as nanosized particles, they had already been used for many years. For instance, Faraday studied gold nanoparticles before their discovery, or the color in colorful glasses came from nanometric clusters of metal oxides [3, 12].

Nanoparticles can be tubes, cylindrical wires, rods, sheets, or even more complicated shapes [9, 11, 20]. They have been employed in various applications, from gene and drug delivery to sensing and catalysis [18, 19, 28]. The synthesis method significantly affects nanomaterials' properties, structure, and chemical composition. Finding a simple, controllable synthesis method that could be commercialized is the first step in fabricating nanostructures with high quality and purity. The various growth methods for nanosized magnetic nanoparticles result in different structures and properties [10].

Nanoparticles may be synthesized through physical or chemical methods. Physical methods include ion sputtering, electron beam evaporation, thermal evaporation, laser evaporation, and plasma evaporation, to name a few. These techniques generally create thin (up to a few dozen nanometers) or thick (up to a few micrometers) layers of nanometric material on a given surface. Chemical methods comprise sol-gel, precipitation or coprecipitation, combustion-based routes like citrate or urea, chemical vapor deposition, microemulsions, hydrothermal processes, and flame-based synthesis, the nanoparticles from which are primarily bulky. These approaches may also be utilized for layer-by-layer production of nanoparticles [25].

Coprecipitation is one of the least expensive and oldest methods. In this method, precursors containing components for nanoparticle formation are dissolved in a suitable solvent. The main components are then precipitated simultaneously by changing the conditions. The precipitate may be obtained from a homogeneous solution through a physical phenomenon such as changing the temperature, solvent type, or evaporating the solvent. However, chemical processes like adding an acid or base or complex-forming reagents are more common. The resultant particles are then separated as precipitates and dried. In some cases, calcination and sintering steps may also be required. The solution composition, the type of solvent, the precipitant, additives, the type of salts in the initial formulation of materials (sulfate, chloride, and so on), pH, the overall process time, temperature, and agitation method are effective parameters involved in the chemical coprecipitation [21, 26, 31].

The synthesis process of magnetite nanoparticles through coprecipitation usually involves destabilizing an acidic solution of Fe^{2+} and Fe^{3+} ions by increasing the pH level. The type and concentration of alkali, the concentration of ferro and ferric salts, Fe(II)/Fe(III) ratio, ionic strength, temperature, mixing method, and agitation efficiency are effective parameters to obtain an average size of 5-14 nm [6].

Dumazet-Bonnamour et al. [8] employed co-precipitated Fe^{2+} and Fe^{3+} in the presence of sodium polyoxyalkylene di-phosphonates. Bocher et al. [4] used Na_2HPO_4. Sun et al. [30] utilized citric acid. Iron chloride salts are usually used for coprecipitation, but Mendoza et al. [17] incorporated ferric nitrate and ammonium oxalate in their study. Iron (III) carboxylate was used by Konishi et al. [13]. Wang et al. [32] carried out the process under a magnetic field and concluded that synthesis efficiency could be increased using a 1T magnetic intensity. Ayala-Valenzuela et al. [2] used common materials (NH_4OH, $FeCl_2$, $FeCl_3$) under particular experimental conditions.

Ma et al. [15] employed common materials but kept the pH values lower than nine and used N_2 as a protective gas. Ordinary materials were utilized by Dresco et al. [7]; however, the temperature range was 4-6 °C. Woltz et al. [33] synthesized magnetite nanoparticles, protected them, and produced composites by melting and quenching $4.9\ Na_2O \cdot 33.3\ CaO \cdot 17.1\ Fe_2O_3 \cdot 44.7\ B_2O_3$. They obtained a uniform Fe_3O_4 precipitate. Bretcanu et al. (Bretcanu et al., 2005) performed a similar study using $Na_2O\text{-}CaO\text{-}SiO_2\text{-}P_2O_5\text{-}FeO\text{-}Fe_2O_3$. Mathur and Venkataramani [16] used nitrate and sulfate salts at high temperatures. Instead of adding an alkali to the solution, Aono et al. [1] added the solution to the alkali. Sun et al. [29] employed Na_2SO_3, which seemed advantageous. Sato et al. [27] boiled the solution and filtered it to separate the powder. Kouassi [14] utilized common substances but increased the temperature to 80 °C.

Combining magnetic nanoparticles with common adsorbents to fabricate magnetic nano adsorbents is one of the applications of magnetic nanoparticles. Nanoadsorbents may be employed to adsorb various pollutants. Nonetheless, separating these adsorbents after adsorbing the pollutants has remained a challenge. Moreover, their regeneration in the desorption process is costly [22, 23, 24]. Adding magnetic nanoparticles to prepare magnetic nanocomposites could resolve these problems. Magnetic nanocomposites can be separated using a strong magnet. Furthermore, when exposed to an alternating magnetic field, these nanoparticles become warm, facilitating their regeneration through desorption.

In this study, several magnetic nanoparticles were synthesized through coprecipitation and characterized using XRD, SEM, and visual observation. Based on the results, the appropriate nanoparticles were selected and combined with activated carbon to obtain magnetic nanoadsorbents. The adsorption capacity of toluene using the as-prepared nanoadsorbents was also investigated.

2. MATERIALS & METHODS

The coprecipitation method was used to synthesize magnetic nanoparticles due to its simplicity and low cost. As shown in Fig. 1a, $FeCl_3.6H_2O$ and $FeSO_4.7H_2O$ were used to prepare magnetite nanoparticles. Ammonium hydroxide (NH_4OH) was employed as the precipitant to form the precipitate phase and magnetite particles. To synthesize 1 g of magnetite Fe_3O_4, 2.3 g $FeCl_3.6H_2O$, and 1.2 g $FeSO_4.7H_2O$ were dissolved in 500 ml water. NH_4OH was then added to the solution dropwise until the pH reached ten and a black precipitate was formed. The precipitates were washed with distilled water, and magnetite nanoparticles were obtained.

Barium hexaferrite nanoparticles were prepared through the steps shown in Fig. 1b. 2.24 g $BaCl_2.2H_2O$ and 2.69 g $FeCl_3.6H_2O$ were dissolved in 500 ml water. The solution pH was increased to 8 using ammonia (Eq. 1). The formed precipitates were separated and dewatered at 375 ºC, followed by curing at 900 ºC for four hours.

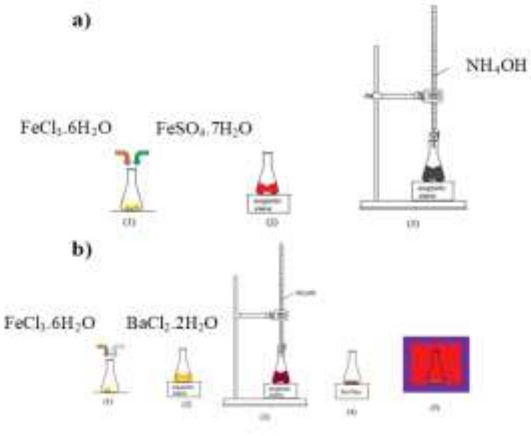

Figure 1. *a) Magnetite nanoparticles synthesis process: 1. Adding reactants, 2. Dissolution of salts, 3. Adding precipitant. b) Barium hexaferrite nanoparticles synthesis process: 1. Addition of reactants, 2. Dissolution of salts, 3. Adding precipitant, 4. Evaporation of undesirable materials, 5. Curation in an autoclave.*

$$12FeCl_3 + BaCl_2 + NH_4OH \rightarrow lOFeOOH, Fe_{2}0_{3}, BaO + NH_4Cl \text{ (room temp)} \quad (1)$$

The resultant substances were heated at 375 ºC for 2.5 h, after which $BaO.Fe_2O_3$ + $5Fe_2O_3$ was produced.

The synthesis of iron nanoparticles was first carried out by using hydrazine. 5 g $FeCl_3.6H_2O$ was dissolved in 100 ml distilled water, and 20 ml hydrazine was added to the solution. Due to the hydrazine's low reduction and H2 production strength, no meaningful result was observed, and iron ions remained in the solution. Hence, another experiment with a different reducing agent was designed. Fig 2.a depicts the experimental steps. 5 g $FeCl_3.6H_2O$ was dissolved in 200 ml distilled water. 1 g $NaBH_4$ was dissolved in 10 ml distilled water, and the resultant mixture was slowly added to the solution containing iron ions. The mixture was agitated using a magnetic stirrer, and a black precipitate formed at the bottom of the container. The extra water was removed, and the precipitate, which was iron particles, was dried at 40 ºC. Finally, the nanoparticles were oxidized to Fe_2O_3 in the laboratory, and no magnetic property was observed.

Given the results mentioned above, a protective coating must have been created on the surface of the iron powder to prevent nanoparticles from oxidization. Given the availability and simplicity of applying silicon alkoxides, coating with SiO_2 was chosen to protect the iron nanoparticles. Fig. 2.b illustrates the overall procedure for coating iron particles with SiO_2. 7 g $FeCl_3.6H_2O$ was first dissolved in 100 ml distilled water. Then, 200 ml ethanol was added to the solution, followed by 10 ml tetraethyl orthosilicate (TEOS). The mixture was agitated for 10 min, after which 2 g of $NaBH_4$ was slowly added to a 50/50 water and alcohol solution. The resultant mixture was dried at 40 ºC for three days.

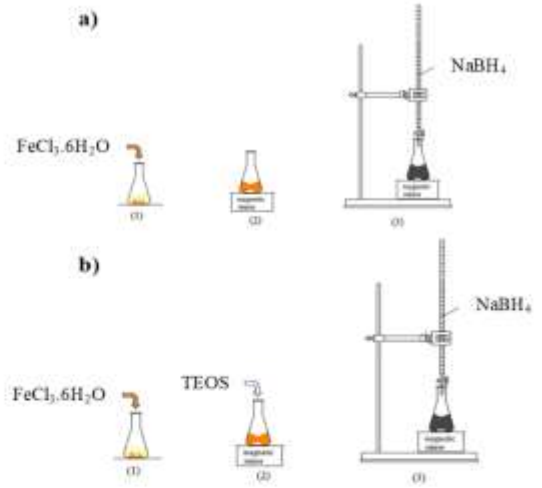

Figure 2. *a) iron nanoparticles synthesis procedure: 1. Adding iron source, 2. Dissolution of iron salt, 3. Adding reducing agent. b) schematic synthesis process of SiO_2-coated iron nanoparticles: 1. Adding iron source, 2. Dissolution of iron salt in ethanol and adding TEOS, 3. Adding reducing agent.*

3. RESULTS & DISCUSSION

3.1. Magnetite Nanoparticles

Fig. 3 shows the X-ray diffraction (XRD) of the magnetite nanoparticles. This figure confirms the formation of the magnetite (Mn) phase. Surface oxidation may have happened due to the particles' small size, resulting in the goethite (Gt) phase formation. As can be observed, the primary peaks are related to the magnetite phase.

The formation of magnetite nanoparticles smaller than 100 nm was confirmed through scanning electron microscopy (SEM), depicted in Fig. 4. This image displays the dimension and geometry of the nanoparticles, and spherical particles in the range of 20-40 nm were obtained.

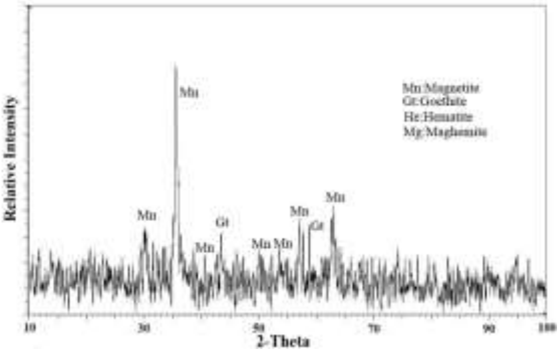

Figure 3. *XRD results for magnetite nanoparticles. An insignificant amount of goethite might be produced due to the ambient conditions.*

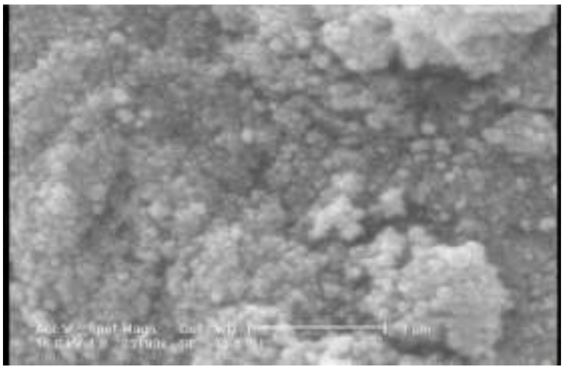

Figure 4. *SEM image of magnetite particles confirmed the formation of <100 nm particles.*

The magnetic properties were investigated, and the results are shown in Fig. 5. As mentioned earlier, the nanoparticles are expected to represent superparamagnetic properties consistent with the obtained results. Given the small size of these nanoparticles (their diameter is lower than the critical diameter, which is nearly 120 nm for magnetite), the energy of the magnetic moment, depending on the crystal network, decreases. Under these conditions, the thermal vibrations of the atoms at the given temperature overcome the existing order, the nanoparticles' moments spin without any resistance, and coercivity is reduced. Considering the more accurate image of the central region, the coercivity value for these magnetite nanoparticles is approximately 35 Oe, which is 3.5 times that of bulky magnetite's coercivity of 10 Oe. Therefore, the magnetite nanoparticles produce more heat when exposed to a variable magnetic field. On the other hand, due to the high specific surface area of the nanoparticles, heat transfer to the stripping bed is faster in the solvent desorption process.

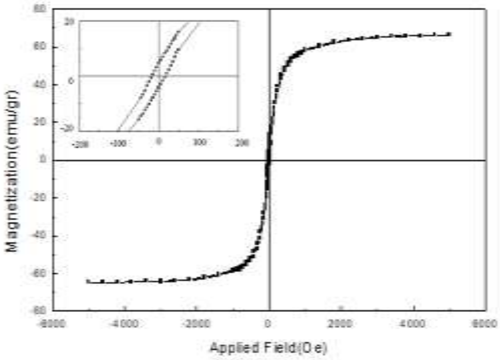

Figure 5. *Magnetic hysteresis loop diagram for synthesized magnetite nanoparticles.*

3.2. Iron Nanoparticles

Elemental iron nanoparticles exhibit outstanding magnetic properties. However, they oxidize quickly under working conditions and lose their magnetic property. The iron nanoparticles prepared in this study had excellent apparent magnetic properties in an aqueous solution, and before drying, they were attracted to the magnet easily (Fig.6-the right image). Nevertheless, they oxidized even at room temperature after drying and no longer had magnetic properties.

Fig. 7. illustrates the apparent magnetic properties of the iron nanoparticles after drying at room temperature. As can be observed, the nanoparticles are not attracted to the magnet due to oxidization. The magnetic properties are significantly reduced when the nanoparticles are coated with SiO_2, as shown in Fig.6.left. Overall, given the obtained results and comparing the coated and uncoated particles qualitatively, the coating process seems to decrease the magnetic properties of the iron nanoparticles. This result aligns with previous studies' findings [1, 16]. Therefore, iron nanoparticles are inappropriate for magnetizing activated carbon.

Figure 6. *Coated and uncoated iron nanoparticles- the right image: uncoated iron nanoparticles are attracted to the magnet quickly; the left picture: coated iron nanoparticles show little tendency towards the magnet.*

Figure 7. *The apparent magnetic properties of iron nanoparticles after being dried at room temperature.*

3.3. Barium Hexaferrite Nanoparticles

The results of the XRD analysis are shown in Fig. 8. The lower spectrum represents the XRD diagram of the product after curing at 375 ºC for 2.5 h, indicating the iron and barium oxides presence.

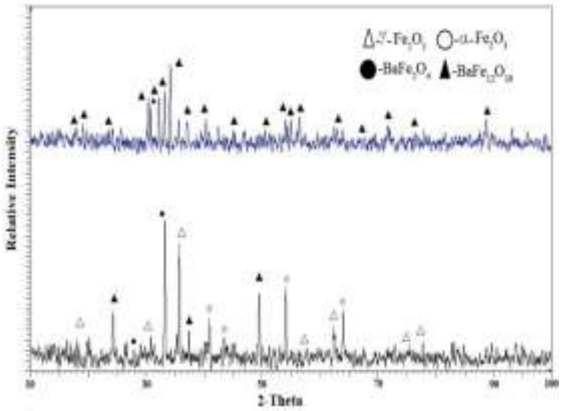

Figure 8. *XRD analysis of the barium hexaferrite production. Lower diagram: after curing at 375 ºC for two hours, which indicates the presence of iron and barium oxides. Upper graph: after curing at 900 ºC for four hours, which confirms the formation of the hexaferrite phase.*

The upper spectrum shows the XRD diagram of the final product after being kept at 900. Given the two-phase diagram of Fe_2O_3 and $2BaO.Fe_2O_3$ and barium to iron ratio of 1:6, heating the product at 900 ºC for four hours led to $BaO.6Fe_2O_3$ confirmed by the XRD analysis. As can be observed, various phases are seen after drying (the lower spectrum), and barium hexaferrite is obtained after heating at 900 ºC and the penetration of barium into the particles.

The synthesized barium hexaferrite nanoparticles' SEM image is shown in Fig. 9. The ordered hexagonal structure is a characteristic of barium hexaferrite. The average size of the nanoparticles is approximately 150 nm.

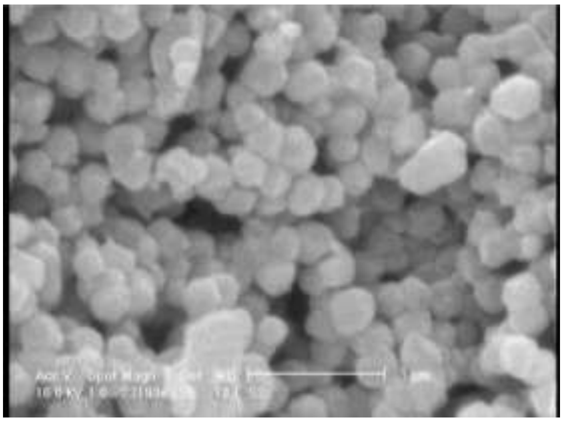

Figure 9. *SEM image of the synthesized barium hexaferrite particles. The ordered crystal structures can be seen clearly.*

As shown in Fig. 10., unlike the magnetite nanoparticles (the upper image), no significant magnetic properties were visually observed when the synthesized barium hexaferrite (the lower image) was exposed to a magnet.

Figure 10. *Visual observations of the magnetite and barium hexaferrite nanoparticle response to a magnetic field. The upper images are related to magnetite nanoparticles, and the lower pictures are related to the barium hexaferrite nanoparticles.*

One of the drawbacks of the coprecipitation method for barium hexaferrite nanoparticle synthesis is that the undesirable salts are left in the final product. These salts are occasionally left with an amorph structure that may not easily be recognized through XRD analysis. Salts such as chlorides and nitrates reduce the diffusion rate and fill the structure's interstitial and substitutional defects, hindering a 100% yield.

Regarding the solubility of barium in neutral aqueous solutions, the salts cannot be removed by washing. If the solution's pH reaches around 8, nearly all the existing barium is solved and washed away. On the other hand, drying the solution in mild temperatures results in the separation of the precipitates. This separation can be recognized through the various colors of the different compounds. Due to these separations after drying, thermal treatment cannot produce a single-phase precipitate. Therefore, using barium hexaferrite nanoparticles in the predicted experimental conditions is unsuitable.

The typical procedure for preparing hexaferrite particles includes mixing barium carbonate with Fe_2O_3 powder and curing at 1200 ºC. The barium atoms diffuse into the structure at this temperature, and after forming the desirable phase, the product is ground to obtain 1 μm particles. These particles have a flat sheet-like shape. Hexaferrites possess an hcp crystal structure where the c axis is perpendicular to the particles' surface. The as-prepared particles may be used in cassette manufacturing.

Several aspects should be considered regarding the synthesis of barium hexaferrite nanoparticles and the importance of the product's high purity in producing significant amounts of heat. First, a strong field must be applied since these particles have a high magnetic moment resistance against spinning (their Hc is high). Moreover, the alternating frequency of the applied magnetic field should be completely controlled to provide the magnetic moments with enough time for spinning. On the other hand, a low alternating frequency reduces the produced heat and causes the yield to decrease.

Given what was mentioned above, many factors affect the heat produced. Considering the visual experiments, the prepared barium hexaferrite particles produce low heat in the experimental conditions. Since improving the experimental conditions, such as increasing the current frequency and intensity, costs considerably, it is not logical to manipulate these factors. On the other hand, given the diffusion mechanism of barium into the structure, using high-temperature furnaces for long periods is not cost-effective.

3.4. Toluene Adsorption

The results of nanoparticle synthesis demonstrated that magnetite nanoparticles are the best option to magnetize activated carbon due to their simple preparation method and strong magnetic properties. Hence, the adsorption potential of toluene on 20% nanoparticles/activated carbon and 50% nanoparticles/ activated carbon nanocomposites was investigated. Fig. 11 illustrates the toluene adsorption capacity of the activated carbon and 20% and 50% magnetic magnetite nanoparticles/activated carbon-based nanocomposites. As can be seen, the adsorption capacity of activated carbon is reduced by 15% and 50% after adding 20% and 50% magnetic magnetite nanoparticles, respectively. Therefore, the 20% nanoparticles/ activated carbon adsorption capacity is acceptable.

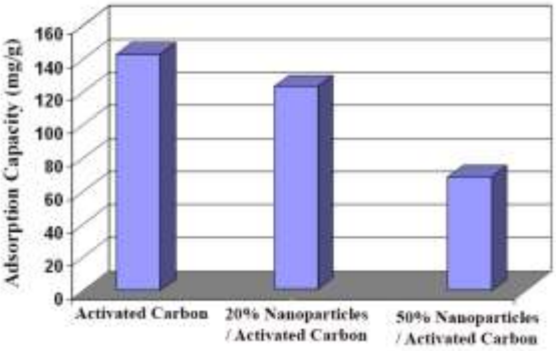

Figure 11. *Toluene adsorption capacity on activated carbon, 20% magnetite nanoparticles/activated carbon, and 50% magnetite nanoparticles/activated carbon nanocomposites.*

4. CONCLUSIONS

The coprecipitation method was employed to prepare magnetite, barium hexaferrite, and coated and uncoated iron-based magnetic nanoparticles. The magnetic properties of the synthesized nanoparticles were investigated using XRD, SEM, and visual observations. The results demonstrated that barium hexaferrite nanoparticles did not have desirable visual magnetic properties, and their fabrication was difficult and expensive. The uncoated iron nanoparticles were unstable and immediately oxidized when exposed to the air, losing their magnetic properties. The coated iron nanoparticles had no prominent magnetic properties. On the other hand, the magnetite nanoparticles had a simple and low-cost production method and showed excellent magnetic properties. The coercivity value for these magnetite nanoparticles was approximately 35 Oe, 3.5 times that of bulky magnetite. Therefore, more heat is produced when the magnetite nanoparticles are exposed to an alternating magnetic field compared to the bulky magnetite. The toluene adsorption results confirmed that the magnetic absorbents from 20% magnetite nanoparticles/activated carbon nanocomposites had acceptable adsorption.

CONFLICT OF INTEREST

The authors declare that they have no conflict of interest.

REFERENCES

1. Aono, H., Hirazawa, H., Naohara, T., Maehara, T., Kikkawa, H., Watanabe, Y., "Synthesis of fine magnetite powder using reverse coprecipitation method and its heating properties by applying AC magnetic field", *Materials Research Bulletin*, 40 (2005) 1126-1135.
2. Ayala-Valenzuela, O., Matutes-Aquino, J., Betancourt-Galindo, R., Garcia-Cerda, L., Fernández, O. R., Fannin, P., Giannitsis, A., "Magnetite-cobalt ferrite nanoparticles for kerosene-based magnetic fluids", *Journal of Magnetism and Magnetic Materials*, 294 (2005) e37-e41.
3. Baghban, A., Sasanipour, J., Pourfayaz, F., Ahmadi, M. H., Kasaeian, A., Chamkha, A. J., Oztop, H. F., Chau, K.-W., "Towards experimental and modeling study of heat transfer performance of water-SiO2 nanofluid in quadrangular cross-section channels", *Engineering Applications of Computational Fluid Mechanics*, 13 (2019) 453-469.
4. Bocher, F., Géhin, A., Ruby, C., Ghanbaja, J., Abdelmoula, M., Génin, J.-M. R., "Coprecipitation of Fe(II–III) hydroxycarbonate green rust stabilised by phosphate adsorption", *Solid State Sciences*, 6 (2004) 117-124.
5. Bretcanu, O., Spriano, S., Verné, E., Cöisson, M., Tiberto, P., Allia, P., "The influence of crystallised Fe3O4 on the magnetic properties of coprecipitation-derived ferrimagnetic glass–ceramics", *Acta Biomaterialia*, 1 (2005) 421-429.
6. Cabuil, V., "*Magnetic Nanoparticles: Preparation and Properties*", Encyclopedia of Surface and Colloid Science, CRC Press, (2015).
7. Dresco, P. A., Zaitsev, V. S., Gambino, R. J., Chu, B., "Preparation and properties of magnetite and polymer magnetite nanoparticles", *Langmuir*, 15 (1999) 1945-1951.
8. Dumazet-Bonnamour, I., Le Perchec, P., "Colloidal dispersion of magnetite nanoparticles via in situ preparation with sodium polyoxyalkylene di-phosphonates", *Colloids and Surfaces A: Physicochemical and Engineering Aspects*, 173 (2000) 61-71.
9. Fard, H. F., Khodaverdi, M., Pourfayaz, F., Ahmadi, M. H., "Application of N-doped carbon nanotube-supported Pt-Ru as electrocatalyst layer in passive direct methanol fuel cell", *International Journal of Hydrogen Energy*, 45 (2020) 25307-25316.
10. Johnson, M., Aloni, S., McCready, D., Bourret-Courchesne, E., "Controlled vapor−liquid−solid growth of indium, gallium, and tin oxide nanowires via chemical vapor transport", *Crystal Growth & Design*, 6 (2006) 1936-1941.
11. Khodaverdi, M., Pourfayaz, F., Mehrpooya, M., "Nitrogen-doped graphene prepared by low-temperature thermal treatment as an electrocatalyst support for methanol oxidation", *Fuel Cells*, 21 (2021) 172-181.
12. Kim, D.-K., Lee, H., Zhang, X., Bae, J.-H., Park, J., "Solvent-dependent electrical characteristics and mechanical stability of flexible organic ferroelectric field-effect transistors", *Micromachines*, 10 (2019) 727.
13. Konishi, Y., Nomura, T., Mizoe, K., "A new synthesis route from spent sulfuric acid pickling solution to ferrite nanoparticles", *Hydrometallurgy*, 74 (2004) 57-65.
14. Kouassi, G. K., Irudayaraj, J., McCarty, G., "Examination of cholesterol oxidase attachment to magnetic nanoparticles", *Journal of Nanobiotechnology*, 3 (2005) 1-9.
15. Ma, M., Zhang, Y., Yu, W., Shen, H.-Y., Zhang, H.-Q., Gu, N., "Preparation and characterization of magnetite nanoparticles coated by amino silane", *Colloids and Surfaces A: Physicochemical and Engineering Aspects*, 212 (2003) 219-226.
16. Mathur, B., Venkataramani, B., "Surface charge and surface chemical characteristics of magnetites substituted with nickel, cobalt and chromium", *Colloids and Surfaces A: Physicochemical and Engineering Aspects*, 140 (1998) 403-416.
17. Mendoza, M., Donado, F., Silva, R., Pérez, M., Carrillo, J., "Magnetite microcrystals for magneto-rheological fluids", *Journal of Physics and Chemistry of Solids*, 66 (2005) 927-931

18. Nami Chemazi, N., Nami, N., Sheikh Bostanabad, A., "Biosynthesis and characterization of Fe3O4/CaO nanoparticles and investigation of its catalytic property", *Journal of Nanostructures*, 12 (2022) 160-169.
19. Nami, N., Lale Mohammadi, S., "One-pot facile synthesis of new 1,2,4-triazolidine derivatives using sodium borohydride and Fe3O4 magnetic nanoparticles (MNPs)", *International Journal of Nanoscience and Nanotechnology*, 13 (2017) 347-357.
20. Nicolae-Maranciuc, A., Chicea, D., Chicea, L. M., "Ag nanoparticles for biomedical applications—Synthesis and characterization—A review", *International Journal of Molecular Sciences*, 23 (2022) 5778.
21. Niculescu, A.-G., Chircov, C., Grumezescu, A. M., "Magnetite nanoparticles: Synthesis methods–A comparative review", *Methods*, 199 (2022) 16-27.
22. Pourfayaz, F., Ahmadi-Avval, P., Haji Tarverdi, M. S., Maleki, A., Ahmadi, M. H., "A study of effects of different surface modifications of MWCNTs on their adsorption capacity of benzene and toluene", *Iranian Journal of Chemistry and Chemical Engineering (IJCCE)*, 36 (2017) 107-114.
23. Pourfayaz, F., Boroun, S., Babaei, J., Ebrahimi Hoseinzadeh, B., "An evaluation of the adsorption potential of MWCNTs for benzene and toluene removal", *International Journal of Nanoscience and Nanotechnology*, 10 (2014) 27-34.
24. Pourfayaz, F., Iranpour, S., Shojaei, O., "Effect of acid treatment of carbon nanotubes on their adsorption capacities of benzene and toluene", *International Journal of Nanoscience and Nanotechnology*, 11 (2015) 219-224.
25. Rana, A., Yadav, K., Jagadevan, S., "A comprehensive review on green synthesis of nature-inspired metal nanoparticles: Mechanism, application and toxicity", *Journal of Cleaner Production*, 272 (2020) 122880.
26. Samrot, A. V., Sahithya, C. S., Selvarani, J., Purayil, S. K., Ponnaiah, P., "A review on synthesis, characterization and potential biological applications of superparamagnetic iron oxide nanoparticles", *Current Research in Green and Sustainable Chemistry*, 4 (2021) 100042.
27. Sato, T., Ishibashi, S., Kimizuka, T., Yamauchi, G., Oshiman, K.-I., "Synthesized ultrafine magnetic minerals and their suppressive effect on the growth of turfgrass mold", *International Journal of Mineral Processing*, 62 (2001) 95-110.
28. Shabani, O., Nami, N., Hajinasiri, R., Hosseinzadeh, M., "Preparation, characterizations, and application of (MWCNTs)-COOH/Fe3O4-CaO hybrid as an effective magnetic catalyst for direct C-glycosylation reactions", *Inorganic and Nano-Metal Chemistry*, (2023) 1-15.
29. Sun, Y.-K., Ma, M., Zhang, Y., Gu, N., "Synthesis of nanometer-size maghemite particles from magnetite", *Colloids and Surfaces A: Physicochemical and Engineering Aspects*, 245 (2004) 15-19.
30. Sun, Y., Duan, L., Guo, Z., Duanmu, Y., Ma, M., Xu, L., Zhang, Y., Gu, N., "An improved way to prepare superparamagnetic magnetite-silica core-shell nanoparticles for possible biological application", *Journal of Magnetism and Magnetic Materials*, 285 (2005) 65-70.
31. Wallyn, J., Anton, N., Vandamme, T. F., "Synthesis, principles, and properties of magnetite nanoparticles for in vivo imaging applications—A review", *Pharmaceutics*, 11 (2019) 601.
32. Wang, J., Zhang, K., Peng, Z., Chen, Q., "Magnetic properties improvement in Fe3O4 nanoparticles grown under magnetic fields", *Journal of Crystal Growth*, 266 (2004) 500-504.
33. Woltz, S., Rüssel, C., "Self-organized nano crystallinity of magnetite precipitated from a 4.9 Na2O· 33.3 CaO· 17.1 Fe2O3· 44.7 B2O3 glass", *Journal of Non-Crystalline Solids*, 337 (2004) 226-231.